



**HAL**  
open science

## A smarter approach to catalysts by design: Combining surface organometallic chemistry on oxide and metal gives selective catalysts for dehydrogenation of 2,3-dimethylbutane

Pascal Rouge, Anthony Garron, Sébastien Norsic, Cherif Larabi, Nicolas Merle, Laurent Delevoye, Régis M. Gauvin, Kai C Szeto, Mostafa Taoufik

### ► To cite this version:

Pascal Rouge, Anthony Garron, Sébastien Norsic, Cherif Larabi, Nicolas Merle, et al.. A smarter approach to catalysts by design: Combining surface organometallic chemistry on oxide and metal gives selective catalysts for dehydrogenation of 2,3-dimethylbutane. *Molecular Catalysis*, 2019, 471, pp.21 - 26. 10.1016/j.mcat.2019.04.011 . hal-03096779

**HAL Id: hal-03096779**

**<https://hal.science/hal-03096779v1>**

Submitted on 6 Jan 2021

**HAL** is a multi-disciplinary open access archive for the deposit and dissemination of scientific research documents, whether they are published or not. The documents may come from teaching and research institutions in France or abroad, or from public or private research centers.

L'archive ouverte pluridisciplinaire **HAL**, est destinée au dépôt et à la diffusion de documents scientifiques de niveau recherche, publiés ou non, émanant des établissements d'enseignement et de recherche français ou étrangers, des laboratoires publics ou privés.

Cite this: DOI: 10.1039/c0xx00000x

www.rsc.org/xxxxxx

ARTICLE TYPE

# A smarter approach to catalysts by design: Combining surface organometallic chemistry on oxide and metal gives selective catalysts for dehydrogenation of 2,3-dimethylbutane

5 Pascal Rouge,<sup>a</sup> Anthony Garron,<sup>a</sup> Sébastien Norsic,<sup>a</sup> Cherif Larabi,<sup>a</sup> Nicolas Merle,<sup>b</sup> Laurent Delevoye,<sup>b</sup> Regis M. Gauvin,<sup>b</sup> Kai C. Szeto,<sup>a,\*</sup> Mostafa Taoufik<sup>a,\*</sup>

Received (in XXX, XXX) Xth XXXXXXXXX 20XX, Accepted Xth XXXXXXXXX 20XX

DOI: 10.1039/b000000x

10 2,3-dimethylbutane is selectively converted into 2,3-dimethylbutenes at 500 °C under hydrogen or 390 °C under nitrogen in the presence of bimetallic catalysts Pt-Sn/Li-Al<sub>2</sub>O<sub>3</sub>. The high stability of the catalyst along the reaction is obtained by selective modification of  $\gamma$ -alumina and platinum nanoparticles using Surface Organometallic Chemistry (SOMC).

Dimethylbutenes are important reagents for both chemical and polymer industries. For example, 2,3-dimethylbutenes is needed for the synthesis of aromatic musks like Tonalide®.<sup>1,2</sup> In the field of polymerization, 2,3-dimethylbutenes are referred as TME and used as crosslinking agents.<sup>3</sup> 2,3-Dimethylbutenes (DMBs = DMB-1 + DMB-2) are provided by the dimerization of propylene over Ni catalysts, known as the Difasol™ process.<sup>4</sup> As the growing global demand for propylene results in the increase of its price, other processes to obtain selectively DMBs have become attractive. These molecules can be obtained through different approaches. We previously reported that tungsten hydride supported on  $\gamma$ -alumina or  $\gamma$ -alumina modified by nickel or silicon allowed to convert isobutene into DMBs at low temperature with high selectivity.<sup>5,6</sup> WOCl<sub>4</sub> supported on silica dehydroxylated at 200 °C followed by alkylation with SnMe<sub>4</sub> achieved excellent performances in isobutene self-metathesis to DMB-2.<sup>7</sup> Another way to product those valuable compounds is the use of well-defined Cu nanoparticles supported on alumina prepared by SOMC which showed high selectivity in hydrogenation of 2,3-dimethylbutadiene to 2,3-dimethylbutenes. This alternative method opens the gate for bio-sourced 2,3-dimethylbutene originated from dehydration of pinacol.<sup>8</sup> In the perspective of an industrial application, 2,3-dimethylbutane is a cheap starting material compared to the corresponding alkenes and can easily be obtained through isomerization of *n*-hexane.<sup>9</sup> The dehydrogenation reaction can be an important way to produce 2,3-dimethylbutenes (DMB-1 and DMB-2) from such readily available starting material.

Most alkane dehydrogenation catalysts are based on supported transition metals. Supported non-noble metals such as chromium or vanadium can be economically advantageous but the obtained selectivity in higher olefins is low due to the cracking reactions. Supported noble metal particles, with or without promoters, have been widely explored.<sup>10</sup> Dehydrogenation catalysts based on platinum are widely used in petrochemistry for example in reforming or in isobutane dehydrogenation to isobutene. Bimetallic PtSn supported on  $\gamma$ -alumina have been extensively used for

dehydrogenation of both light and higher hydrocarbons. Many studies showed that the presence of Sn has an important effect on the selectivity and inhibits sintering of Pt clusters allowing to improve the stability of the catalyst towards deactivation by coking, and prevents hydrocracking, hydrogenolysis and isomerisation reactions.<sup>11-16</sup>

Indeed, the addition of alkali metals as promoters allows neutralizing the surface acidity and inhibiting the isomerisation reaction of hydrocarbon. Other studies reported that alkali metals might promote H<sub>2</sub> spillover and inhibit coke deposition.<sup>17-22</sup> In most cases, the bimetallic catalysts are prepared by the classical methods (successive impregnation, co-impregnation and sol-gel) of platinum and tin salts.<sup>23-27</sup> Nevertheless, the impregnation procedure does not lead to the exclusive formation of bimetallic particles. The co-existence of isolated tin and platinum monometallic phase may give low selectivity in desired product in particular for the dehydrogenation of hexanes by isomerization and aromatization reactions.<sup>27,28</sup> Preparation techniques play a significant role in controlling the type of materials obtained. Surface organometallic chemistry on oxide (SOMC/Oxide) and metals (SOMC/M) leads to well-defined bimetallic catalysts whose active sites have high homogeneity in their nature.<sup>8</sup> On the other hand, improving selectivity also requires inhibiting the acid-catalyzed reactions on the support (cracking, isomerization, aromatization and polymerization). A most common method is to introduce additives, such as basic alkaline elements.

The reaction of a tin organometallic compound with metallic surfaces has been pioneered by Yermakov and Ryndin in the 1970s.<sup>29,30</sup> This surface organometallic chemistry approach has been extensively studied in our laboratory for isobutane dehydrogenation. In fact platinum and rhodium nanoparticles carried on silica have been successfully modified by tin or germanium.<sup>31-34</sup> The latter synthetic approach affords selective localisation of the Sn or Ge atoms on the Pt nanoparticles, as previously confirmed by Mössbauer and EXAFS spectroscopies. The resulting catalysts, prepared by SOMC on metal, display high selectivity and stability during isobutane dehydrogenation under hydrogen due to well-defined bimetallic Pt-Sn phase. In the literature, there are only few examples reporting the selective dehydrogenation of 2,3-dimethylbutane.<sup>35-37</sup> However, no example reports the conversion of 2,3-dimethylbutane into 2,3-dimethylbutenes on  $\gamma$ -alumina supported bimetallic PtSn catalyst prepared by SOMC.

In this paper, we demonstrate a stable and selective catalyst for the dehydrogenation of dimethylbutanes to 2,3-

dimethylbutenes based on Pt nano-particles supported on alumina. Furthermore, different promoting agents have been employed through the SOMC methodology on alumina and on the platinum nanoparticle in order to identify the most performing catalyst.

In order to leverage our previous characterizations of alumina and alumina-supported catalysts, we selected as a support a  $\gamma$ -alumina (EVONIK) with a BET surface area of  $100 \text{ m}^2\text{g}^{-1}$  that had been partially dehydroxylated in vacuum at  $500 \text{ }^\circ\text{C}$  ( $\text{Al}_2\text{O}_{3-500}$ ). Its remaining surface hydroxyl groups, with a density of about  $2.0 \text{ OH per nm}^2$  ( $0.65 \text{ mmol g}^{-1}$ ), are potential sites for reaction with organometallic complexes.<sup>38</sup> The reaction of  $\text{Al}_2\text{O}_{3-500}$  with a toluene solution containing  $\text{Pt}(\text{acac})_2$  (relative to the surface hydroxyl concentration) at room temperature affords a surface-modified alumina bearing Pt moieties, after washing of the excess of Pt precursor. IR spectroscopy indicates that grafting of  $\text{Pt}(\text{acac})_2$  proceeds at least partially on different surface hydroxyl groups (Fig. 1). Resolved peaks at  $1400$ ,  $1530$ ,  $1580$  and  $1600 \text{ cm}^{-1}$  have previously been assigned to  $\delta(\text{C-H})$ ,  $\nu(\text{C-C})$  and  $\nu(\text{C=O})$  for grafted and physisorbed acac ligands, respectively.<sup>39</sup> The presence of alkyl groups is further confirmed by  $\nu(\text{C-H})$  at  $3000\text{-}2800 \text{ cm}^{-1}$ . However, the O-H region ( $3800\text{-}3200 \text{ cm}^{-1}$ ) is un-resolved, suggesting the presence of multiple interactions between the remaining Al-OH groups and the surface organic and/or organometallic fragments. Elemental analysis revealed that the Pt loading was  $2 \text{ wt}\%$ .

$^1\text{H}$  magic angle spinning (MAS) NMR spectrum of the latter material is presented on Figure 2a. It comprises several signals stemming from the surface Pt-acac fragments and from aluminum hydroxyl groups. For the sake of comparison, the  $^1\text{H}$  MAS NMR spectrum of the support,  $\gamma\text{-Al}_2\text{O}_{3-500}$ , is shown on Figure 2b. Thus, the spectrum of  $\text{Pt}(\text{acac})_2$  supported on alumina features a characteristic signal at  $5.4 \text{ ppm}$ , accounting for C-H acac protons. From the  $^1\text{H}\text{-}^1\text{H}$  DQ-SQ MAS NMR spectrum (Fig. 3), which reveals spatial proximities, the acac methyl groups were located in the  $2.4\text{-}1.7 \text{ ppm}$  region, as the acac C-H signal at  $5.4 \text{ ppm}$  displays correlations with protons at such chemical shifts. As expected from the assignment, the methinic CH does not give rise to a self-correlation. Regarding the AlOH network signals ( $4.5\text{-}0.5 \text{ ppm}$ ), the doubly bridging hydroxyl signal is rather unperturbed, at about  $2.2\text{-}1.6 \text{ ppm}$ . On the other hand, the terminal hydroxyl groups are significantly affected by the grafting. Indeed, the intensity of the

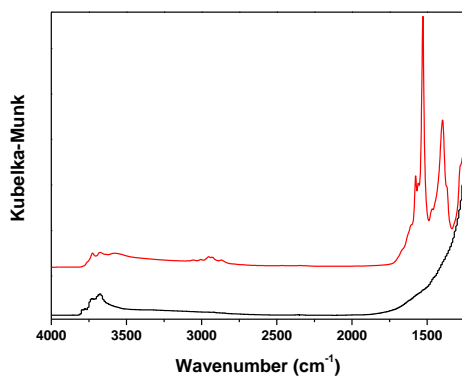


**Fig. 1** DRIFT spectrum of  $\text{Pt}(\text{acac})_2$  after reaction with  $\gamma\text{-Al}_2\text{O}_3$  in toluene at room temperature.

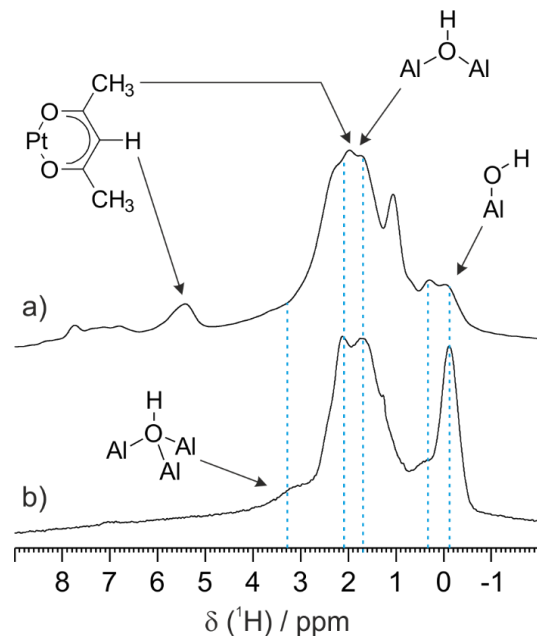


**Fig. 2**  $^1\text{H}$  MAS NMR spectrum of a)  $\text{Pt}(\text{acac})_2$  supported on alumina and b)  $\gamma\text{-Al}_2\text{O}_{3-500}$  (800 MHz, spinning speed 20 kHz).

peak at  $-0.2 \text{ ppm}$  (accounting for terminal hydroxyls on tetracoordinated aluminum centers)<sup>40</sup> is markedly lower compared to that of the pristine sample (Figure 2a). This indicates that reaction occurred with these sites. Interestingly, a new rather sharp signal at  $1.1 \text{ ppm}$  is now observed. This could be due to Pt-coordinated Al-OH group, for which the bonding on the metal would induce a  $1 \text{ ppm}$  increase of the chemical shift. In addition,

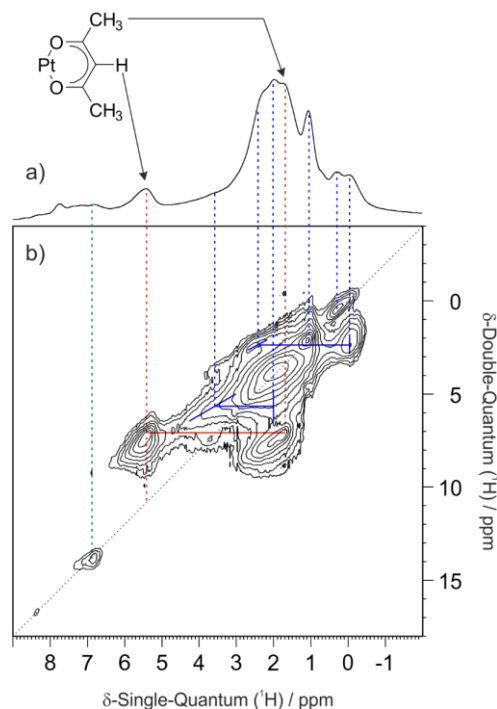


**Fig. 3** a)  $^1\text{H}$  MAS NMR and b)  $^1\text{H}\text{-}^1\text{H}$  DQ-SQ MAS NMR spectra (800 MHz, spinning speed 20 kHz); Red lines : signals related to Pt-acac ; Blue lines : signals related to alumina hydroxyls ; Green lines : signals related to olefinic by-products.

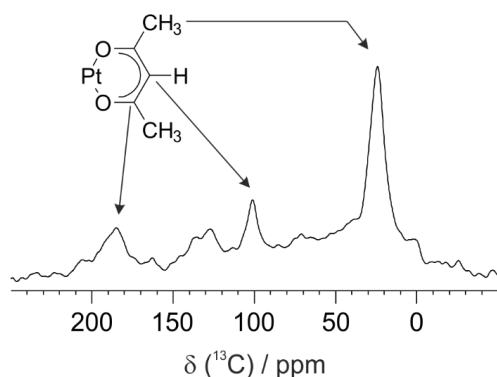


**Fig. 4**  $^{13}\text{C}$  CP MAS NMR spectrum of  $\text{Pt}(\text{acac})_2$  supported on alumina (100.6 MHz, spinning speed 10 kHz)

weak signals are detected at high chemical shifts (about 7 ppm), which are assigned to physisorbed by-products originating from the grafting reaction, in agreement with observation on the IR spectrum. The  $^{13}\text{C}$  CP (Cross Polarization) MAS NMR spectrum (Figure 4) comprises peaks accounting for Pt-bound acac groups, at 184 (C-O), 101 (CH) and 24 ppm ( $\text{CH}_3$ ), which compares well with the data for  $\text{Pt}(\text{acac})_2$  (186, 103 and 25 ppm).

The resulting material was reduced under  $\text{H}_2$  at 550 °C leading to supported  $\text{Pt}/\text{Al}_2\text{O}_3$  catalyst (2 wt%). The DRIFT spectrum revealed disappearance of the C-H fragments (Fig. S1). The particle size distribution of this monometallic catalyst has been determined by TEM analysis (Fig. S2). The distribution (in surface) is rather narrow with an average particle diameter close to 2.3 nm. The average dispersion of the metallic particles is then close to 45 %, according to the literature.<sup>41,42</sup>

When 2,3-dimethylbutane (DMBH) dehydrogenation is performed over  $\text{Pt}/\text{Al}_2\text{O}_3$  in a dynamic flow reactor (200 mg  $\text{Pt}/\text{Al}_2\text{O}_3$ ,  $T = 500$  °C,  $P_{\text{total}} = 1$  bar,  $P_{\text{DMBH}} = 350$  mbar and flow rate = 10  $\text{ml}\cdot\text{min}^{-1}$ ), the reaction gives an initial maximal conversion of 28% before decreasing to 18% in 30 h (Fig. 5a). The product selectivities, provided in Fig. S3, are mainly branched hexenes (42.1%), branched hexanes (24.4%) and methane (10.7%). The minor products are composed of benzene, pentanes, pentenes, butanes, butenes, propane,

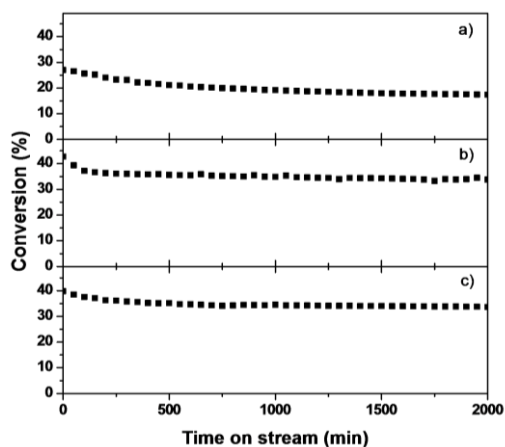
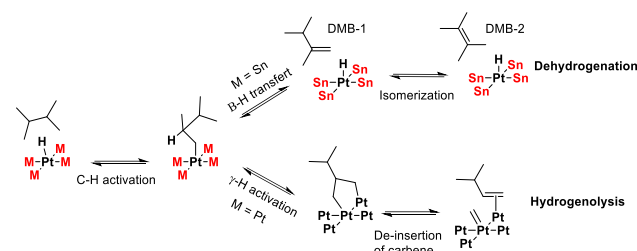


**Fig. 5** Conversion of DMBSH on a)  $\text{Pt}/\text{Al}_2\text{O}_3$ ; b)  $\text{Pt}/\text{Li}-\text{Al}_2\text{O}_3$ ; and c)  $\text{PtSn}/\text{Li}-\text{Al}_2\text{O}_3$ , 200 mg,  $P_{\text{DMBH}} = 350$  mbar, 10 ccm of  $\text{H}_2$ , 500 °C

propene and ethane (See Table S1). The formation of



**Scheme 1.** Side reactions provided by  $\gamma$ -H activation

isopentene and methane can be explained by C-H activation of DMBSH followed by  $\gamma$ -H activation on adjacent platinum site and de-insertion of carbene (Scheme 1).<sup>43-46</sup> The main unsaturated acyclic  $\text{C}_6$  components are DMBs with a fairly high relative selectivity (69.6%,  $\text{DMB-2}/\text{DMB-1} = 2.06$ ) obtained by dehydrogenation of dimethylbutane accompanied with isohexenes (or methylpentenes) 10.5%, neohexene 10.4% and dimethylbutadiene 9.5% (See Table 1 and Fig. S4). The formation of neohexene and methylpentenes is due to isomerisation reaction on the acidic site of alumina.<sup>47</sup> Benzene is a result of aromatisation of DMBD either on acidic sites of alumina<sup>48</sup> or on platinum surface.<sup>49</sup> This reaction induces the formation of coke, which explains the deactivation of the catalyst. The formation of hexane isomers and smaller compounds is due to isomerisation and cracking reaction occurring on the acidic sites of alumina.<sup>50</sup> These results are confirmed by a blank reaction with alumina alone under the same reaction conditions (Fig. S5). We observe that the conversion of dimethyl-butane (DMBH) is 14%, and the products are propane 39.9%, methane 21.5%, hexenes 9.3%, ethane 6.6%, butanes 7.6%, pentenes 4.2%, pentanes 3.6%, hexanes 3.5%, dimethylbutadiene 1.5% and traces of propylene and benzene (Fig. S6).

In order to limit these side reactions, poisoning of the acidic site by an excess lithium has been studied. The reaction between *n*-butyl-lithium in hexane and dehydroxylated  $\gamma$ -alumina at 500 °C at room temperature gives a new support ( $\text{Li}-\text{Al}_2\text{O}_3$ ). Li content was 2.8 wt%. Quantitative gas chromatography (GC) analysis of gas phase showed the presence of *n*-BuH, which originated from protolysis of Bu-Li by Al-OH from alumina. DRIFT displayed adsorption bands in the regions characteristic for aliphatic C-H fragments (Fig. S7). Moreover, the  $^1\text{H}$  MAS and  $^{13}\text{C}$  CP MAS NMR (Figures S8) data confirmed the presence of alumina-physisorbed BuLi based on  $^1\text{H}$  NMR peaks at 0.1, 0.8 and 1.2 ppm,  $^{13}\text{C}$  NMR peaks at -1.1, 11.4, 18.5, 28.8 ppm (Figure S9) and  $^7\text{Li}$  MAS NMR signal at 0.6 ppm attributed to  $\equiv\text{Al}-\text{O}-\text{Li}^+$  and BuLi physisorbed (Figure S10).<sup>51, 52</sup> The resulting modified  $\text{Li}/\text{Al}_2\text{O}_3$  was calcinated under air at 500 °C and exposed to DMBSH under

**Table 1** Relative selectivity in among unsaturated hexenes for the conversion of 2,3-DMBSH on the catalyst, 200 mg, 10 ccm of  $\text{H}_2$ , 500 °C.

Catalysts	DMB1	DMB2	Neohexene	Isohexenes	DMBD
$\text{Pt}/\text{Al}_2\text{O}_3$	22.7	46.9	10.4	10.5	9.5
$\text{Pt}/\text{Li}-\text{Al}_2\text{O}_3$	45.9	51.5	-	-	2.6
$\text{PtSn}/\text{Li}-\text{Al}_2\text{O}_3$	42.9	52.9	0.5	0.5	3.2
$\text{PtGe}/\text{Li}-\text{Al}_2\text{O}_3$	29.2	61.0	5.1	3.3	1.4

the same conditions as before. No noticeable activity (Fig. S4, ESI) was observed.

Pt/Li-Al<sub>2</sub>O<sub>3</sub> catalyst (2 wt% Pt) was prepared by grafting of platinum acetylacetonate in toluene at room temperature on the new support Li-Al<sub>2</sub>O<sub>3</sub> followed by reduction under hydrogen at 550 °C (Fig. S6., ESI). DRIFT spectra after grafting of Pt(acac)<sub>2</sub> shows resolved peaks at 1400, 1530, 1580 and 1600 cm<sup>-1</sup> previously assigned to δ(C-H), ν(C-C) and ν(C=O) for grafted Pt-acetylacetonate fragment and physisorbed Li(acac) respectively. This later salt is obtained by substitution reaction of AlO-Li with Pt-acac fragments. The presence of alkyl groups is further confirmed by ν(C-H) at 3000-2800 cm<sup>-1</sup>. The reduction at 550 °C under hydrogen (Figure S11) show the disappearance of all bands attributed to Pt complex on support. Elemental analysis revealed that the Pt loading was 2 wt%. The particle size distribution of this monometallic catalyst Pt/Li-Al<sub>2</sub>O<sub>3</sub> has been determined by TEM analysis (Figure S12). The distribution (in surface) is rather narrow with an average particle diameter close to 1.5 nm. The average dispersion of the metallic particles of Pt/Li-Al<sub>2</sub>O<sub>3</sub>, determined by (O<sub>2</sub>-H<sub>2</sub>)-titration, is higher (70%) than Pt/Al<sub>2</sub>O<sub>3</sub> (45%). This result indicate the importance of particle-support interaction on particle size.

When DMBH dehydrogenation is performed in a dynamic flow reactor (200 mg Pt/Li-Al<sub>2</sub>O<sub>3</sub>, T = 500 °C, P = 1 bar, P<sub>DMBH</sub> = 350 mbar and flow rate = 10 ml.min<sup>-1</sup>), the reaction gives an initial maximal conversion of 43% and then reaches 36% after 30h of reaction (Fig. 5b). This improvement of the catalyst activity is related to the elevated dispersion obtained after the lithiation of the surface. The product selectivities are 51.6% in hexenes and 20.9% in methane. The remaining products correspond to a mixture of benzene, hexanes, pentanes, pentenes, butanes, propane, propene and ethane (Table S1 and Fig. S13).

Only traces of isomerisation of 2,3-dimethylbutane and 2,3-dimethylbutenes is observed on Pt/Li-Al<sub>2</sub>O<sub>3</sub> compared to Pt/Al<sub>2</sub>O<sub>3</sub> (other hexanes 24.4 %). The main unsaturated C<sub>6</sub> components are DMBs with high relative selectivity (97.4%, DMB-2/DMB-1 = 1.12), obtained by dehydrogenation of dimethylbutane, accompanied with small quantity of DMBD (Fig. S14).

These results indicate that the introduction of lithium on the support has virtually eliminated alkane isomerization reactions. On the other hand, the fact that the dispersion is higher has simultaneously raised the selectivity of methane, that originates from total hydrogenolysis of DMBH.

In order to overcome the former reaction, modification of the platinum surface by tin and germanium via Surface Organometallic Chemistry (SOMC) has been performed. In fact, the addition of tin or germanium may decrease the presence of adjacent platinum atoms and then overcome the γ-H activation and also the aromatization reaction.<sup>49</sup> The monometallic catalyst Pt/Li-Al<sub>2</sub>O<sub>3</sub> was mixed with an excess either Sn(n-C<sub>4</sub>H<sub>9</sub>)<sub>4</sub> or HGe(n-C<sub>4</sub>H<sub>9</sub>)<sub>3</sub> in heptane at 80 °C for 24h under hydrogen. In the case of the tin-modified system, the gas production is followed by gas chromatography in order to determine the complete deposition of tin into platinum atoms after 24 h (BuH/Pt<sub>S</sub> = 3, Pt<sub>S</sub> = platinum on surface of particles). Elemental analysis gives 1.32 wtSn%, 2 wtPt% and 2.8 wtLi%

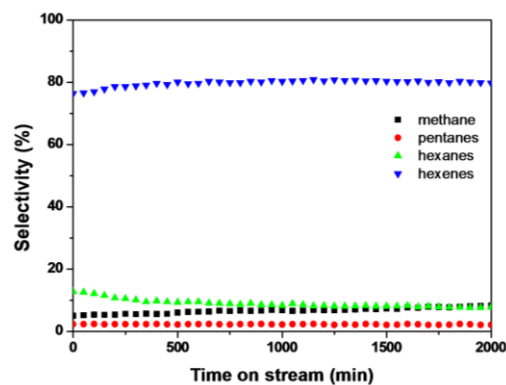


**Fig. 6** Time-resolved evolution of the selectivity of products on PtSn/Li-Al<sub>2</sub>O<sub>3</sub>, 200 mg, P<sub>DMBH</sub> = 350 mbar, 10 ccm of H<sub>2</sub>, 500 °C. Traces (< 1%) have been omitted for clarity.

(Sn/Pt<sub>total</sub> = 1.09). The particle size distribution of this catalyst has been determined by TEM analysis (Fig. S15). The distribution (in surface) is rather narrow with an average particle diameter close to 1.5 nm. This result confirms that the SOMC methodology does not modify the morphology of the nanoparticles. After modification the hydrogen uptake during H<sub>2</sub>/O<sub>2</sub>/H<sub>2</sub> titration drops from 86 to 60 μmol.g<sup>-1</sup> confirming the selective modification of the platinum surface by tin.

Under the same conditions, the catalyst modified by tin has been evaluated in DMBH dehydrogenation. The corresponding conversion in function of time is presented in Fig. 5c. After an initial drop of conversion, the activity remains stable for 30h (conversion = 34%). In presence of the bimetallic PtSn/Li-Al<sub>2</sub>O<sub>3</sub> catalyst, the absolute selectivity in desired products (DMB-1 and DMB-2) is high (77%) compared to what is obtained with Pt/Li-Al<sub>2</sub>O<sub>3</sub> (50.2%) (Fig. 6 and Table S1). The relative selectivity in DMBs is very high (95.8%). These results showed that the modifications of Pt/Al<sub>2</sub>O<sub>3</sub> by both Li and Sn increase the selectivity in the desired products with high stability in function of the time. This catalyst dehydrogenates of DMBH to DMBs in high selectivity (Table 1 and Fig. 7).

The influence of addition of Ge within the Pt particles on the catalytic performance was also probed. When DMBH dehydrogenation is performed in a dynamic flow reactor in the same conditions over PtGe/Li-Al<sub>2</sub>O<sub>3</sub>, the reaction gives an

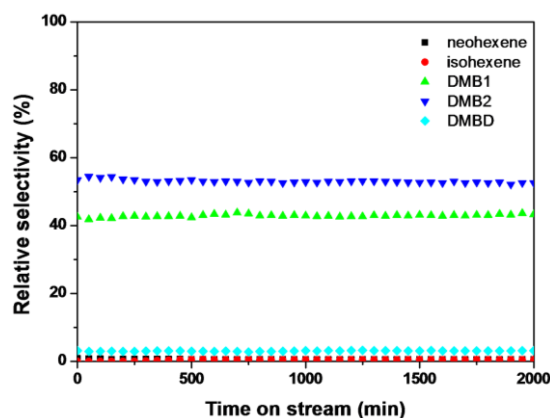


**Fig. 7** Time-resolved evolution of relative selectivity of acyclic C<sub>6</sub> on PtSn/Li-Al<sub>2</sub>O<sub>3</sub>, 200mg, P<sub>DMBH</sub> = 350 mbar, 10ccm of H<sub>2</sub>, 500°C.

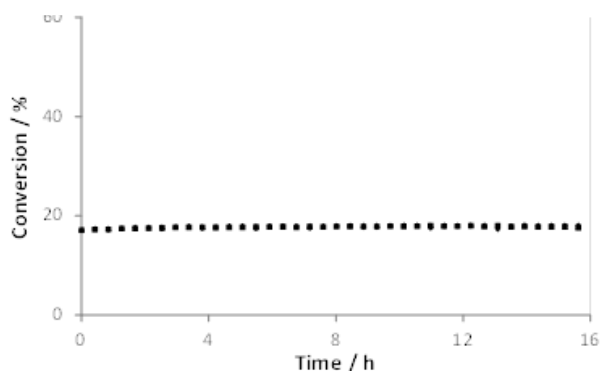


**Fig. 8** Conversion of 2,3-DMBH on PtSn/Li-Al<sub>2</sub>O<sub>3</sub>, 100mg, saturation pressure, 5ccm of N<sub>2</sub>, 390°C.

initial maximal conversion of 44% before to reach 36% after 30 h of reaction (Fig. S16). The absolute selectivity in hexenes is 53.5% (Fig. S17), with small amounts of methylpentenes and neohexene (Table S1 and Fig. S18). This behaviour might be related to an ability of PtGe/Li-Al<sub>2</sub>O<sub>3</sub> to perform the isomerisation of DMB-1. In addition, the catalyst seems to deactivate contrary to PtSn/Li-Al<sub>2</sub>O<sub>3</sub>.

The PtSn/Li-Al<sub>2</sub>O<sub>3</sub> catalyst demonstrates a high stability (up to 65 h, Fig. S19) and high selectivity to DMBs under hydrogen. This was further investigated at different temperatures (Fig S20).

Thermodynamic predicts that the conversion will decrease with the temperature. In fact the observed conversions are 31, 13 and 7% at 500, 460 and 430°C, respectively. This behaviour is related to the presence of hydrogen in feed which disfavoured the dehydrogenation reaction.<sup>53</sup> However, decrease of temperature improves the formation of 2,3-dimethylbutenes among the unsaturated C<sub>6</sub>, which reach a value of 99.8% (Table S2) at 430°C. Nevertheless, production of methane as well as pentanes and propane increases when the temperature drops. Those compounds are originated from the  $\gamma$ -H activation which is favoured in excess of hydrogen and low temperature. Hydrogen was initially used to limit the cracking reaction. However, at fairly low temperature, such as 430 °C, cracking reactions are almost negligible. Hence, hydrogen was replaced by an inert gas and both the activity and selectivity are expected to be improved. Moreover, substituting hydrogen with an inert gas, for example nitrogen, will reduce the economic and safety issues.

For this purpose the bimetallic PtSn/Li-Al<sub>2</sub>O<sub>3</sub> catalyst has been evaluated under nitrogen (Fig. 8). At 390°C under nitrogen the conversion value is below the equilibrium. At this temperature, the catalyst remains stable. Hence, hydrogen can be substituted by nitrogen with an important benefit. Importantly, the catalyst gives 100% hexenes (DMB-1 = 46.1%; DMB-2 = 51.9%). The only by-product of the reaction is DMBD (2%). The thus developed bimetallic platinum-tin catalyst on lithiated alumina presents high activity and selectivity with high stability in function of time.

In conclusion, controlled modification of the Pt/alumina by lithium and tin using new approach based on SOMC on metal and oxide in consecutive steps allowed to enhance the productivity, the stability and the selectivity in valuable branched hexenes, in particular DMBs. Importantly, the catalyst can operate under inert atmosphere at fairly low temperature without deactivation, providing large benefit in

terms of efficiency and safety. The field of application of this new material will be extended to other alkanes in the near future, in particular to the conversion of neohexane into neohexene, an important intermediate in fragrance industry.

## Notes and references

- <sup>a</sup> Université Lyon 1, Institut de Chimie de Lyon; CPE Lyon; CNRS, UMR 5265 C2P2, LCOMS; Bâtiment 308 F 43 Blvd du 11 Novembre 1918 F-69616, Villeurbanne Cedex, France. Fax: (+33) (0)4 72 43 17 95; E-mail: [taoufik@cpe.fr](mailto:taoufik@cpe.fr); [kai.szeto@cpe.fr](mailto:kai.szeto@cpe.fr)
- <sup>b</sup> Univ. Lille, CNRS, Centrale Lille, ENSCL, Univ. Artois, UMR 8181 - UCCS - Unité de Catalyse et Chimie du Solide, F-59000 Lille, France ; e-mail : [regis.gauvin@univ-lille.fr](mailto:regis.gauvin@univ-lille.fr)
- <sup>†</sup>Electronic Supplementary Information (ESI) available: preparation, characterisation of catalysts and catalytic test procedure. See DOI: 10.1039/b000000x/
1. H. Mimoun, *Chimia*, 1996, **50**, 620-625.
2. H. Sato, H. Tojima and K. Ikimi, *J. Mol. Catal. A-Chem.*, 1999, **144**, 285-293.
3. C. P. Reyneke-Barnard, M. H. S. Gradwell and W. J. McGill, *J. Appl. Polym. Sci.*, 2000, **78**, 1100-1111.
4. H. Olivier-Bourbigou, L. Magna and D. Morvan, *Appl. Catal. A-Gen.*, 2010, **373**, 1-56.
5. A. Garron, F. Stoffelbach, N. Merle, K. C. Szeto, J. Thivolle-Cazat, J. M. Basset, S. Norsic and M. Taoufik, *Catal. Sci. Technol.*, 2012, **2**, 2453-2455.
6. N. Merle, F. Stoffelbach, M. Taoufik, E. Le Roux, J. Thivolle-Cazat and J. M. Basset, *Chem. Commun.*, 2009, 2523-2525.
7. Y. Bouhoute, A. Garron, D. Grekov, N. Merle, K. C. Szeto, A. De Mallmann, I. Del Rosal, L. Maron, G. Girard, R. M. Gauvin, L. Delevoeye and M. Taoufik, *ACS Catal.*, 2014, **4**, 4232-4241.
8. K. Boukebbous, N. Merle, C. Larabi, A. Garron, W. Darwich, E. A. Laifa, K. Szeto, A. De Mallmann and M. Taoufik, *New J. Chem.*, 2017, **41**, 427-431.
9. K. An, S. Alayoglu, N. Musselwhite, K. Na and G. A. Somorjai, *J. Am. Chem. Soc.*, 2014, **136**, 6830-6833.
10. J. Sattler, J. Ruiz-Martinez, E. Santillan-Jimenez and B. M. Weckhuysen, *Chem. Rev.*, 2014, **114**, 10613-10653.
11. R. D. Cortright, J. M. Hill and J. A. Dumesic, *Catal. Today*, 2000, **55**, 213-223.
12. J. M. Hill, R. D. Cortright and J. A. Dumesic, *Appl. Catal. A-Gen.*, 1998, **168**, 9-21.
13. H. Lieske, A. Sarkany and J. Volter, *Appl. Catal.*, 1987, **30**, 69-80.
14. B. M. Nagaraja, C. H. Shin and K. D. Jung, *Appl. Catal. A-Gen.*, 2013, **467**, 211-223.
15. A. Virnovskaia, S. Morandi, E. Rytter, G. Ghiotti and U. Olsbye, *J. Phys. Chem. C*, 2007, **111**, 14732-14742.
16. J. Wu, Z. M. Peng and A. T. Bell, *J. Catal.*, 2014, **311**, 161-168.
17. S. A. Bocanegra, A. A. Castro, A. Guerrero-Ruiz, O. A. Scelza and S. R. de Miguel, *Chem. Eng. J.*, 2006, **118**, 161-166.
18. M. L. Casella, G. J. Siri, G. F. Santori, O. A. Ferretti and M. M. Ramirez-Corredores, *Langmuir*, 2000, **16**, 5639-5643.
19. S. R. De Miguel, S. A. Bocanegra, I. M. J. Vilella, A. Guerrero-Ruiz and O. A. Scelza, *Catal. Lett.*, 2007, **119**, 5-15.
20. G. J. Siri, G. R. Bertolini, M. L. Casella and O. A. Ferretti, *Mater. Lett.*, 2005, **59**, 2319-2324.
21. M. Tasbihi, F. Feyzi, M. A. Amlashi, A. Z. Abdullah and A. R.

- Mohamed, *Fuel Process. Technol.*, 2007, **88**, 883-889.
22. Y. W. Zhang, Y. M. Zhou, J. J. Shi, S. J. Zhou, X. L. Sheng, Z. W. Zhang and S. M. Xiang, *J. Mol. Catal. A-Chem.*, 2014, **381**, 138-147.
- 5 23. O. A. Bariãs, A. Holmen and E. A. Blekkan, in *Catalyst Deactivation 1994*, 1994, vol. 88, pp. 519-524.
24. G. T. Baronetti, S. R. Demiguel, O. A. Scelza, M. A. Fritzler and A. A. Castro, *Appl. Catal.*, 1985, **19**, 77-85.
25. R. Burch and L. C. Garla, *J. Catal.*, 1981, **71**, 360-372.
- 10 26. H. Lieske and J. Volter, *J. Catal.*, 1984, **90**, 96-105.
27. B. A. Sexton, A. E. Hughes and K. Foger, *J. Catal.*, 1984, **88**, 466-477.
28. G. Meitzner, G. H. Via, F. W. Lytle, S. C. Fung and J. H. Sinfelt, *J. Phys. Chem.*, 1988, **92**, 2925-2932.
- 15 29. E. N. Yurchenko and V. I. Kuznetsov, *React. Kinet. Catal. Lett.*, 1983, **23**, 113-117.
30. V. I. Zaikovskii, V. I. Kovalchuk, Y. A. Ryndin, L. M. Plyasova, B. N. Kuznetsov and Y. I. Yermakov, *React. Kinet. Catal. Lett.*, 1980, **14**, 99-103.
- 20 31. O. A. Ferretti, G. J. Siri, F. Humblot, J. P. Candy, B. Didillon and J. M. Basset, *React. Kinet. Catal. Lett.*, 1998, **63**, 115-120.
32. F. Humblot, J. P. Candy, F. Le Peltier, B. Didillon and J. M. Basset, *J. Catal.*, 1998, **179**, 459-468.
33. F. Humblot, D. Didillon, F. Lepeltier, J. P. Candy, J. Corker, O. Clause, F. Bayard and J. M. Basset, *J. Am. Chem. Soc.*, 1998, **120**, 137-146.
- 25 34. E. Tena, J. P. Candy, M. F. Cornil, B. Jousseume, M. Spagnol and J. M. Basset, *J. Mol. Catal. A-Chem.*, 1999, **146**, 53-64.
- 35 35. N. Homs, J. Llorca, M. Riera, J. Jolis, J. L. G. Fierro, J. Sales and P. R. de la Piscina, *J. Mol. Catal. A-Chem.*, 2003, **200**, 251-259.
- 30 36. S. B. Kogan and M. Herskowitz, *Ind. Eng. Chem. Res.*, 2002, **41**, 5949-5951.
37. M. Nakamura, M. Yamada and A. Amano, *J. Catal.*, 1975, **39**, 125-133.
- 35 38. M. Delgado, C. C. Santini, F. Delbecq, R. Wischert, B. Le Guennic, G. Tosin, R. Spitz, J. M. Basset and P. Sautet, *J. Phys. Chem. C*, 2010, **114**, 18516-18528.
39. M. Womes, T. Cholley, F. Le Peltier, S. Morin, B. Didillon and N. Szydłowski-Schildknecht, *Appl. Catal. A-Gen.*, 2005, **283**, 9-22.
- 40 40. M. Taoufik, K. C. Szeto, N. Merle, I. Del Rosal, L. Maron, J. Trebosc, G. Tricot, R. M. Gauvin and L. Delevoye, *Chem.-Eur. J.*, 2014, **20**, 4038-4046.
41. G. Dalmai-Imelik, C. Leclercq and I. Mutin, *J. Microsc.-Oxf.*, 1974, **20**, 123-&.
- 45 42. Vanharde.R and F. Hartog, *Surf. Sci.*, 1969, **15**, 189-&.
43. J. R. Anderson and N. R. Avery, *J. Catal.*, 1966, **5**, 446-&.
44. F. Garin and F. G. Gault, *J. Am. Chem. Soc.*, 1975, **97**, 4466-4476.
45. M. Leconte, *J. Mol. Catal.*, 1994, **86**, 205-220.
46. W. T. Osterloh, M. E. Cornell and R. Pettit, *J. Am. Chem. Soc.*, 50 1982, **104**, 3759-3761.
47. C. S. John, C. Kemball and R. A. Rajadhyaksha, *J. Catal.*, 1979, **57**, 264-271.
48. Y. Q. Song, X. X. Zhu, S. J. Xie, Q. X. Wang and L. Y. Xu, *Catal. Lett.*, 2004, **97**, 31-36.
- 55 49. A. A. Susu, *J. Chem. Technol. Biotechnol.*, 2008, **83**, 928-942.
50. I. Surjo and E. Christoffel, *J. Catal.*, 1979, **60**, 133-139.
51. D. Seebach, R. Haessig and J. Gabriel, *Helvetica Chimica Acta*, 1983, **66**, 308-337.
52. J. F. McGarrity and C. A. Ogle, *J. Am. Chem. Soc.*, 1985, **107**, 1805-1810.
- 60 53. T. Waku, J. A. Biscardi and E. Iglesia, *J. Catal.*, 2004, **222**, 481-492.